Gravitational lensing in the strong field limit

V. Bozza*
Dipartimento di Fisica "E.R. Caianiello", Università di Salerno, Italy.
Istituto Nazionale di Fisica Nucleare, Sezione di Napoli.
(Dated: February 6, 2008)

We provide an analytic method to discriminate among different types of black holes on the ground of their strong field gravitational lensing properties. We expand the deflection angle of the photon in the neighbourhood of complete capture, defining a strong field limit, in opposition to the standard weak field limit. This expansion is worked out for a completely generic spherically symmetric spacetime, without any reference to the field equations and just assuming that the light ray follows the geodesics equation. We prove that the deflection angle always diverges logarithmically when the minimum impact parameter is reached. We apply this general formalism to Schwarzschild, Reissner-Nordstrom and Janis-Newman-Winicour black holes. We then compare the coefficients characterizing these metrics and find that different collapsed objects are characterized by different strong field limits. The strong field limit coefficients are directly connected to the observables, such as the position and the magnification of the relativistic images. As a concrete example, we consider the black hole at the centre of our galaxy and estimate the optical resolution needed to investigate its strong field behaviour through its relativistic images.

PACS numbers: 95.30.Sf, 04.70.Bw, 98.62.Sb
Keywords: Relativity and gravitation; Classical black holes; Gravitational lensing

I. INTRODUCTION

Gravitational lensing is one of the first applications of General Relativity ever studied [1]. Firstly it was recognized in the light deflection by sun, secondly in lensing of quasars by foreground galaxies, then in the formation of giant arcs in galaxy clusters and finally in galactic microlensing. Now it is an ordinary phenomenon in the panorama of astronomical observations (see [2] for a complete treatment and references therein).

The full theory of gravitational lensing has been developed following the scheme of the weak field approximation and, in this formulation, it has been successfully employed to explain all the physical observations.

In the last years, however, the scientific community is starting to look at this phenomenon from the opposite point of view, opening a strong field perspective. Viergutz [3] made a semi-analytical investigation about geodesics in Kerr geometry; in Ref. [4] the appearance of a black hole in front of a uniform background was studied; Falcke, Melia and Agol [5] considered the emission of the accretion flow as source. Virbhadra & Ellis [6] showed that a source behind a Schwarzschild black hole would produce one set of infinite relativistic images on each side of the black hole. These images are produced when a light ray with small impact parameter winds one or several times around the black hole before emerging. Later on, by an alternative formulation of the problem, Frittelli, Kling & Newman [7] attained an exact lens equation, giving integral expressions for its solutions, and compared their results to those by Virbhadra & Ellis. The same problem has been investigated by Bozza et al. in Ref. [8], where a strong field limit was first defined in Schwarzschild black hole lensing and used to find the position and the characteristics of all the relativistic images analytically. Eiroa, Romero and Torres [9] applied the same technique to a Reissner - Nordstrom black hole. Recently, in another work [10], Virbhadra & Ellis distinguished the main features of gravitational lensing by normal black holes and by naked singularities, analyzing the Janis, Newman, Winicour metric. They remarked the importance of these studies in providing a test for the cosmic censorship hypothesis.

The reason for such an interest in gravitational lensing in strong fields is that by the properties of the relativistic images it may be possible to investigate the regions immediately outside of the event horizon. High resolution imaging of black holes by VLBI [11] could be able to detect the relativistic images and retrieve information about strong fields stored within these new observables. Moreover, since alternative theories of gravitation must agree with GR in the weak field limit, in order to show deviations from GR it is necessary to probe strong fields in some way. Indeed, deviation of light rays in strong fields is one of the most promising grounds where a theory of gravitation can be tested in its full form.

Of course, the study of null geodesics in strong fields is not easy and up to now it has always been carried out using numerical techniques. An analytical treatment would enlighten the dependence of the observables on the parameters of the system, allow easy checks about the detectability of the images and open the way to comparisons between the results in different metrics. In Ref. [8], a new way to expand the deflection angle in the Schwarzschild metric was suggested. The deflection angle near its divergence was approximated by its leading order and its first regular term and then plugged into the

*Electronic address: valboz@sa.infn.it

lens equation. In this way, very simple and reliable analytical formulae were derived for the relativistic images and their main features.

So, as the weak field limit takes the first order deviation from Minkowski, the strong field limit starts from complete capture of the photon and takes the leading order in the divergence of the deflection angle.

The strong field limit of Ref. [8] was only developed in Schwarzschild spacetime. In this paper, we provide a general method to extend the strong field limit to a generic static spherically symmetric spacetime. Our method is universal and can be applied to any spacetime in any theory of gravitation, provided that photons satisfy the standard geodesics equation. The parameters of the strong field limit expansion are directly connected with the observables, providing an effective tool to discriminate among different metrics. In Sect. 2, we state the problem and carry out the strong field limit of the deflection angle. In Sect. 3, we apply the method to some simple metrics: Schwarzschild, Reissner-Nordstrom and Janis-Newman-Winicour black hole, discussing their differences with reference to the gravitational lensing phenomenology. In Sect. 4, we establish a connection between the strong field limit coefficients and the relativistic images, analyzing the case of the black hole at the center of our galaxy as a concrete example where our results can be tested. Finally, Sect. 5 contains the summary.

II. STRONG FIELD EXPANSION OF THE DEFLECTION ANGLE

A generic spherically symmetric spacetime has line-element [13]

$$ds^2 = A(x)dt^2 - B(x)dx^2 - C(x)\left(d\theta^2 + \sin^2\theta\phi^2\right). \quad (1)$$

where

$$\begin{aligned} A(x) &\overset{x\to\infty}{\Longrightarrow} 1 - \tfrac{2M}{x} \\ B(x) &\overset{x\to\infty}{\Longrightarrow} 1 + \tfrac{2M}{x} \\ C(x) &\overset{x\to\infty}{\Longrightarrow} x^2, \end{aligned} \quad (2)$$

in order to correctly match the weak gravitational field far from the lensing object.

We require that the equation

$$\frac{C'(x)}{C(x)} = \frac{A'(x)}{A(x)}. \quad (3)$$

admits at least one positive solution. We shall call the largest root of Eq. (3) the radius of the photon sphere x_m (for an alternative definition of the photon sphere, see [12]). A, B, C, A' and C' must be positive for $x > x_m$

For metrics expressed in standard coordinates ($C(x) = x^2$) a sufficient condition for the existence of x_m is the presence of a static limit (a radius x_s such that $A(x_s) = 0$). Our strong field expansion takes the photon sphere as the starting point. In our study, therefore, we shall not consider naked singularities without a photon sphere. For a numerical study of this situation, see Ref. [10].

A photon incoming from infinity with some impact parameter u, will be deviated while approaching the black hole. It will reach a minimum distance x_0 and then emerge in another direction. Of course, the approach phase is identical to the departure phase, with the time reversed.

By the conservation of the angular momentum, the closest approach distance is related to the impact parameter u by

$$u = \sqrt{\frac{C_0}{A_0}}. \quad (4)$$

where the subscript 0 indicates that the function is evaluated at x_0.

From the geodesics equation it is easy to extract the quantity

$$\frac{d\phi}{dx} = \frac{\sqrt{B}}{\sqrt{C}\sqrt{\frac{C}{C_0}\frac{A_0}{A} - 1}} \quad (5)$$

which gives the angular shift of the photon as a function of the distance from the center (see [13] for the complete derivation).

The deflection angle can then be calculated as a function of the closest approach:

$$\alpha(x_0) = I(x_0) - \pi \quad (6)$$

$$I(x_0) = \int_{x_0}^{\infty} \frac{2\sqrt{B}dx}{\sqrt{C}\sqrt{\frac{C}{C_0}\frac{A_0}{A} - 1}}. \quad (7)$$

It is easy to check that for a vanishing gravitational field ($A = B = 1$, $C = x^2$) $\alpha(x_0)$ identically vanishes. In the weak field limit, the integrand is expanded to the first order in the gravitational potential. This limit is no longer valid when the closest approach distance significantly differs from the impact parameter (which, by Eq. (4), means that $A(x_0)$ significantly differs from 1 and/or $C(x_0)$ from x_0^2, i.e. the photon passes in a strong gravitational field).

When we decrease the impact parameter (and consequently x_0), the deflection angle increases. At some point, the deflection angle will exceed 2π, resulting in a complete loop around the black hole. Decreasing u further, the photon will wind several times before emerging. Finally, for $x_0 = x_m$ (see Sect. II A), corresponding to an impact parameter $u = u_m$, the deflection angle diverges and the photon is captured (see Fig. 1).

In this section, we will show that this divergence is logarithmic for all spherically symmetric metrics. Our purpose is to get an analytical expansion of the deflection angle close to the divergence in the form

$$\alpha(x_0) = -a\log\left(\frac{x_0}{x_m} - 1\right) + b + O\left(x_0 - x_m\right), \quad (8)$$

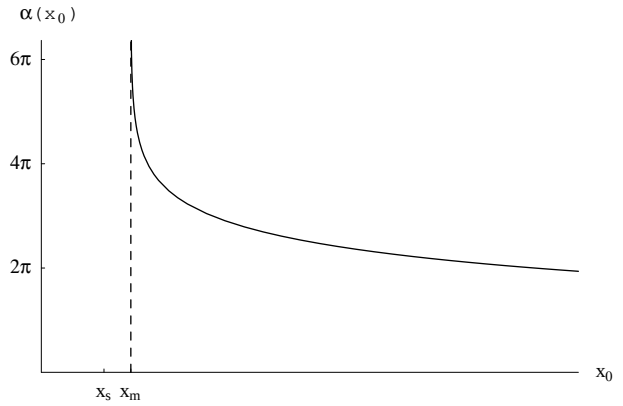

FIG. 1: General behaviour of the deflection angle as a function of the closest approach x_0. The deflection angle increases as x_0 decreases and diverges at $x_0 = x_m$. Each time $\alpha(x_0)$ reaches a multiple of 2π, the photon completes a loop before emerging.

where all the coefficients depend on the metric functions evaluated at x_m.

As the angular separation of the image from the lens is $\theta = \frac{u}{D_{OL}}$, where D_{OL} is the distance between the lens and the observer, we need to express the deflection angle in terms of this variable. So, we shall finally transform Eq.(8) to

$$\alpha(\theta) = -\overline{a}\log\left(\frac{\theta D_{OL}}{u_m} - 1\right) + \overline{b} + O\left(u - u_m\right) \tag{9}$$

which we define as the *strong field limit* of the deflection angle. The rest of this section is devoted to the calculation of the two coefficients a and b in a first step and then of $\overline{a}$ and $\overline{b}$.

A. Divergent term of the deflection angle

We define two new variables

$$y = A(x) \tag{10}$$

$$z = \frac{y - y_0}{1 - y_0} \tag{11}$$

where $y_0 = A_0$. The integral (7) in the deflection angle becomes

$$I(x_0) = \int_0^1 R(z, x_0) f(z, x_0) dz \tag{12}$$

$$R(z, x_0) = \frac{2\sqrt{By}}{CA'}\left(1 - y_0\right)\sqrt{C_0} \tag{13}$$

$$f(z, x_0) = \frac{1}{\sqrt{y_0 - \left[\left(1 - y_0\right)z + y_0\right]\frac{C_0}{C}}} \tag{14}$$

where all functions without the subscript 0 are evaluated at $x = A^{-1}\left[\left(1 - y_0\right)z + y_0\right]$.

The function $R(z, x_0)$ is regular for all values of z and x_0, while $f(z, x_0)$ diverges for $z \to 0$. To find out the order of divergence of the integrand, we expand the argument of the square root in $f(z, x_0)$ to the second order in z:

$$f\ \ (z, x_0) \sim f_0(z, x_0) = \frac{1}{\sqrt{\alpha z + \beta z^2}} \tag{15}$$

$$\alpha\ = \frac{1 - y_0}{C_0 A_0'}\left(C_0' y_0 - C_0 A_0'\right) \tag{16}$$

$$\beta\ = \frac{\left(1 - y_0\right)^2}{2C_0^2 {A_0'}^3}\Big[2C_0 C_0' {A_0'}^2 + \\ + \left(C_0 C_0'' - 2{C_0'}^2\right) y_0 A_0' - C_0 C_0' y_0 A_0''\Big]. \tag{17}$$

When α is non zero, the leading order of the divergence in f_0 is $z^{-1/2}$, which can be integrated to give a finite result. When α vanishes, the divergence is z^{-1} which makes the integral diverge. Examining the form of α, we see that it vanishes at $x_0 = x_m$, with x_m defined by Eq. (3). Each photon having $x_0 < x_m$ is captured by the central object and cannot emerge back.

To solve the integral (12), we split it into two pieces

$$I(x_0) = I_D(x_0) + I_R(x_0), \tag{18}$$

where

$$I_D(x_0) = \int_0^1 R(0, x_m) f_0(z, x_0) dz \tag{19}$$

contains the divergence and

$$I_R(x_0) = \int_0^1 g(z, x_0) dz \tag{20}$$

$$g(z, x_0) = R(z, x_0) f(z, x_0) - R(0, x_m) f_0(z, x_0). \tag{21}$$

is the original integral with the divergence subtracted. We shall solve both integrals separately and then sum up their results to rebuild the deflection angle. Here we deal with I_D and its divergence, while in the next subsection we shall verify that I_R is indeed regular.

The integral $I_D(x_0)$ can be solved exactly, giving

$$I_D(x_0) = R(0, x_m)\frac{2}{\sqrt{\beta}}\log\frac{\sqrt{\beta} + \sqrt{\alpha + \beta}}{\sqrt{\alpha}}. \tag{22}$$

Since we are interested in the terms up to $O(x_0 - x_m)$, we expand α as

$$\alpha = \frac{2\beta_m A_m'}{1 - y_m}\left(x_0 - x_m\right) + O\left(x_0 - x_m\right)^2, \tag{23}$$

where

$$\beta_m = \beta|_{x_0 = x_m} = \frac{C_m\left(1 - y_m\right)^2\left(C_m'' y_m - C_m A''(x_m)\right)}{2y_m^2 {C_m'}^2} \tag{24}$$

and substitute in $I_D(x_0)$. Rearranging all terms, we find

$$I_D(x_0) = -a \log\left(\frac{x_0}{x_m} - 1\right) + b_D + O(x_0 - x_m), \quad (25)$$

$$a = \frac{R(0, x_m)}{\sqrt{\beta_m}} \quad (26)$$

$$b_D = \frac{R(0, x_m)}{\sqrt{\beta_m}} \log \frac{2(1 - y_m)}{A'_m x_m}. \quad (27)$$

Eq. (25) yields the leading order in the divergence of the deflection angle, which is logarithmic, as anticipated before. The coefficient a of Eq. (8) is then given by Eq. (26).

B. Regular term of the deflection angle

In order to find the correct coefficient b in Eq. (8), we have to add to the term b_D coming from Eq. (27), an analogous term coming from the regular part of the original integral, defined by Eq. (20).

We can expand $I_R(x_0)$ in powers of $(x_0 - x_m)$

$$I_R(x_0) = \sum_{n=0}^{\infty} \frac{1}{n!}(x_0 - x_m)^n \int_0^1 \frac{\partial^n g}{\partial x_0^n}\bigg|_{x_0 = x_m} dz \quad (28)$$

and evaluate the single coefficients.

If we had not subtracted the singular part from $R(z, x_0) f(z, x_0)$, we would have an infinite coefficient for $n = 0$, while all other coefficients would be finite. However, the function $g(z, x_0)$ is regular in $z = 0, x_0 = x_m$ as can be easily checked by a power expansion, recalling that $\alpha_m = 0$.

Since we are interested to terms up to $O(x_0 - x_m)$, we will just retain the $n = 0$ term

$$I_R(x_0) = \int_0^1 g(z, x_m) dz + O(x_0 - x_m) \quad (29)$$

and then

$$b_R = I_R(x_m) \quad (30)$$

is the term we need to add to b_D in order to get the regular coefficient. Recalling also the term $-\pi$ in the deflection angle, we have

$$b = -\pi + b_D + b_R. \quad (31)$$

The coefficient b_R can be easily evaluated numerically for all metrics, since the integrand has no divergence. However, in many cases it is also possible to build a completely analytical formula for b_R as well. In fact, in Schwarzschild metric, the integral (29) is solved exactly (see Sect. III A). Then, in most metrics, we can expand Eq. (29) in powers of their parameters, starting from the Schwarzschild limit, and evaluate each coefficient separately. This is what we shall do for Reissner-Nordstrom and Janis-Newman-Winicour black holes (see Sect. III).

C. From $\alpha(x_0)$ to $\alpha(\theta)$

From Eq. (4), we see that the minimum impact parameter is

$$u_m = \sqrt{\frac{C_m}{y_m}}. \quad (32)$$

Expanding Eq. (4), we find

$$u - u_m = c\,(x_0 - x_m)^2 \quad (33)$$

$$c = \frac{C''_m y_m - C_m A''_m}{4\sqrt{y_m^3 C_m}} = \beta_m \sqrt{\frac{y_m}{C_m^3}} \frac{{C'_m}^2}{2\,(1 - y_m)^2}. \quad (34)$$

Using this relation, we can write the deflection angle as a function of θ:

$$\alpha(\theta) = -\overline{a} \log\left(\frac{\theta D_{OL}}{u_m} - 1\right) + \overline{b} \quad (35)$$

$$\overline{a} = \frac{a}{2} = \frac{R(0, x_m)}{2\sqrt{\beta_m}} \quad (36)$$

$$\overline{b} = b + \frac{a}{2} \log \frac{c x_m^2}{u_m} = -\pi + b_R + \overline{a} \log \frac{2\beta_m}{y_m}. \quad (37)$$

This concludes our general discussion of the form of the deflection angle in the strong field limit. Even if the proof is somewhat tricky, the application to concrete cases is very straightforward, as we shall see in Sect. III. In fact, once we write a metric, it is sufficient to:

- solve Eq. (3) to find x_m;
- write β_m from Eq. (24) and $R(0, x_m)$ from Eq. (13);
- compute b_R from Eq. (30) numerically or by a proper expansion in the parameters of the metric;
- compute the coefficients u_m, $\overline{a}$ and $\overline{b}$ from Eqs. (32), (36) and (37), respectively.

The crucial step is the calculation of b_R, since it is the only integral involved in the whole procedure.

III. APPLICATIONS

In this section, we apply the general formulation of the strong field limit to three simple examples. First, we shall revisit Schwarzschild spacetime, whose strong field limit gravitational lensing has already been studied in Ref. [8]. Then we will apply our method to Reissner-Nordstrom spacetime, which was explored numerically in Ref. [9]. Finally, as an example of extended theory of gravitation, we shall consider a Janis, Newman, Winicour black hole, whose strong field limit expansion has not been investigated so far. In all three cases, we shall derive analytical formulae for the strong field limit coefficients, in order to analyze the functional dependences of the deflection angle on the parameters of the metrics.

A. Schwarzschild lensing

This is the simplest spherically symmetric metric describing the outer solution for a black hole. It only depends on the mass of the central object (by Birkhoff's theorem). It is convenient to define the Schwarzschild radius $x_s = 2M$ as the measure of distances; then, in standard coordinates, the functions in the metric become

$$A(x) = 1 - \frac{1}{x} \tag{38}$$

$$B(x) = \left(1 - \frac{1}{x}\right)^{-1} \tag{39}$$

$$C(x) = x^2, \tag{40}$$

which obviously satisfy all hypotheses required in Sect. II, with static limit $x_s = 1$.

The two functions $R(z, x_0)$ and $f(z, x_0)$ read

$$R(z, x_0) = 2 \tag{41}$$

$$f(z, x_0) = \frac{1}{\sqrt{\left(2 - \frac{3}{x_0}\right) z + \left(\frac{3}{x_0} - 1\right) z^2 - \frac{z^3}{x_0}}}. \tag{42}$$

From Eqs. (16), (17), or directly from the expansion of the denominator of f, we read off the coefficients α and β

$$\alpha = 2 - \frac{3}{x_0} \tag{43}$$

$$\beta = \frac{3}{x_0} - 1. \tag{44}$$

The equation $\alpha = 0$ defines the radius of the photon sphere

$$x_m = \frac{3}{2}. \tag{45}$$

Consequently, $\beta_m = 1$.

In this simple case, it is possible to solve the integral in Eq. (30) exactly and write the regular term in the deflection angle

$$b_R = 2 \log\left[6\left(2 - \sqrt{3}\right)\right] = 0.9496. \tag{46}$$

From Eqs. (36) and (37), we derive the coefficients $\overline{a}$, $\overline{b}$ and u_m of the deflection angle

$$\overline{a} = 1 \tag{47}$$

$$\overline{b} = -\pi + b_R + \log 6 = -0.4002 \tag{48}$$

$$u_m = \frac{3\sqrt{3}}{2}. \tag{49}$$

Then the Schwarzschild deflection angle, in the strong field limit, is

$$\alpha(\theta) = -\log\left(\frac{2\theta D_{OL}}{3\sqrt{3}} - 1\right) + \log\left[216\left(7 - 4\sqrt{3}\right)\right] - \pi, \tag{50}$$

as obtained in Ref. [8].

In this simple case, we can compare the exact deflection angle $\alpha_{ex}(\theta)$, calculated numerically and the strong field limit $\alpha_{app}(\theta)$. The most external image appears where $\alpha(\theta)$ falls below 2π. This happens at $u - u_m = 0.003264$. Here the discrepancy between α_{ex} and α_{app} is about 0.06%, which corresponds to an error in the position of the outer image of the order 0.4%. With such a high accuracy, we are encouraged to take the Schwarzschild strong field limit as the starting point for successive series expansions to evaluate b_R in more advanced metrics.

B. Reissner-Nordstrom lensing

Reissner-Nordstrom metric describes the gravitational field of a spherically symmetric massive object endowed with an electric charge q. The metric functions in standard coordinates are

$$A(x) = 1 - \frac{1}{x} + \frac{q^2}{x^2} \tag{51}$$

$$B(x) = \left(1 - \frac{1}{x} + \frac{q^2}{x^2}\right)^{-1} \tag{52}$$

$$C(x) = x^2. \tag{53}$$

They satisfy the hypotheses required in Sect. II, only when $q \leq \frac{3}{4\sqrt{2}}$. However, beyond the critical value $q = 0.5$, there is no event horizon and causality violations appear [14, 15]. We shall restrict to $q < 0.5$.

The coefficients α and β are

$$\alpha = \left(2 - \frac{3}{x_0} + \frac{4q^2}{x_0^2}\right) \frac{x_0 - q^2}{x_0 - 2q^2} \tag{54}$$

$$\beta = \left(\frac{3}{x_0} - 1 - \frac{9q^2}{x_0^2} + \frac{8q^4}{x_0^3}\right) \frac{x_0 \left(x_0 - q^2\right)^2}{\left(x_0^3 - 2q^2\right)^3} \tag{55}$$

which reduce to the Schwarzschild coefficients when $q \longrightarrow 0$. From the equation $\alpha = 0$, we derive the radius of the photon sphere

$$x_m = \frac{3}{4}\left(1 + \sqrt{1 - \frac{32q^2}{9}}\right), \tag{56}$$

which yields

$$\beta_m = \left[-9 + 32q^2 - 144q^4 + 512q^6 + \sqrt{9 - 32q^2} \cdot \left(3 + 16q^2 - 80q^4\right)\right] \left[8\left(q - 4q^3\right)\right]^{-2}. \tag{57}$$

The regular term b_R cannot be calculated analytically, but we can expand the integrand in (29) in powers of q and evaluate the single coefficients. We get

$$b_R = b_{R,0} + b_{R,2} q^2 + O(q^4), \tag{58}$$

where $b_{R,0}$ is the value of the coefficient for an uncharged black hole, calculated in the previous subsection and

given by Eq. (46); the correction is quadratic in the charge q of the black hole. Its coefficient is

$$b_{R,2} = \frac{8}{9}\left\{\sqrt{3} - 4 + \log\left[6\left(2-\sqrt{3}\right)\right]\right\} = -1.5939. \tag{59}$$

It is very easy to calculate further terms in the expansion of b_R, deriving analytical formulae which prove to be very accurate even for large values of q.

Following Sect. II, we calculate the coefficients for the formula of the deflection angle

$$\overline{a} = \frac{x_m\sqrt{x_m - 2q^2}}{\sqrt{(3-x_m)\,x_m^2 - 9q^2x_m + 8q^4}} \tag{60}$$

$$\overline{b} = -\pi + b_R + \overline{a}\log 2\left(x_m - q^2\right)^2 \cdot \cdot\frac{\left[(3-x_m)\,x_m^2 - 9q^2x_m + 8q^4\right]}{\left(x_m - 2q^2\right)^3\left(x_m^2 - x_m + q^2\right)} \tag{61}$$

$$u_m = \frac{\left(3+\sqrt{9-32q^2}\right)^2}{4\sqrt{2}\sqrt{3-8q^2+\sqrt{9-32q^2}}}. \tag{62}$$

In [9], the coefficients a and b were calculated numerically. Here, by our general method, we have been able to derive the coefficient $\overline{a}$ for the logarithmic divergence exactly and find a formula for $\overline{b}$ which is valid up to second order in q, indicating the way to extend it to an arbitrary order.

We notice that the radius of the photon sphere x_m decreases as the charge increases, but becomes imaginary only for $q = \frac{3}{4\sqrt{2}} > \frac{1}{2}$; i.e., even when there is no horizon, a photon can be captured by the gravitational field of a hypothetical object with a charge greater than the critical value.

In Fig. 2, we evaluate the deflection angle at $u = u_m + 0.003$ as a function of q. The plot shows that, just using the first correction to b_R, we get an excellent approximation to the deflection angle. In fact, we see that up to $q = 0.3$, the error in the position of the outer image, calculated using the strong field limit, stays below 4%.

Finally, in Fig. 3, we plot the coefficients of the strong field limit as functions of q, calculating the full $\overline{b}$ numerically. We see that $\overline{a}$ and $\overline{b}$ deviate from the corresponding Schwarzschild values as the charge increases. As we shall see in Sect. IV, the strong field limit coefficients are directly connected to the observables. It is then possible, in principle, to distinguish a Reissner-Nordstrom black hole from a Schwarzschild black hole, using strong field gravitational lensing.

C. Janis-Newman-Winicour lensing

The spherically symmetric solution to the Einstein massless scalar equations ($R_{\mu\nu} = \Phi_{,\mu}\Phi_{,\nu}$, $\Phi^{;\mu}_{;\mu}$) can be written in Janis-Newman-Winicour (JNW) coordinates

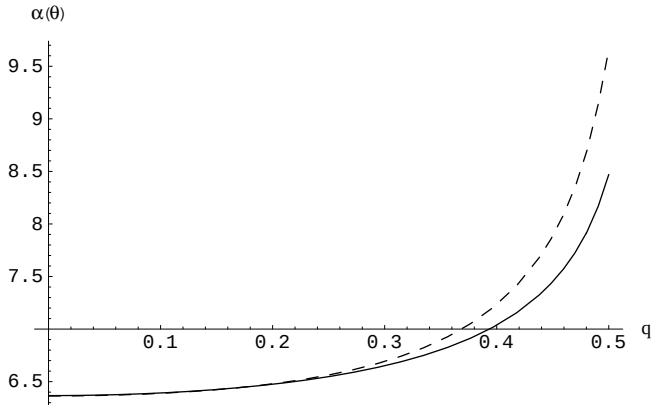

FIG. 2: Deflection angles in Reissner-Nordstrom metric evaluated at $u = u_m + 0.003$ as functions of q. The solid line is the exact deflection angle; the dashed line is the strong field limit with b_R truncated to second order in q.

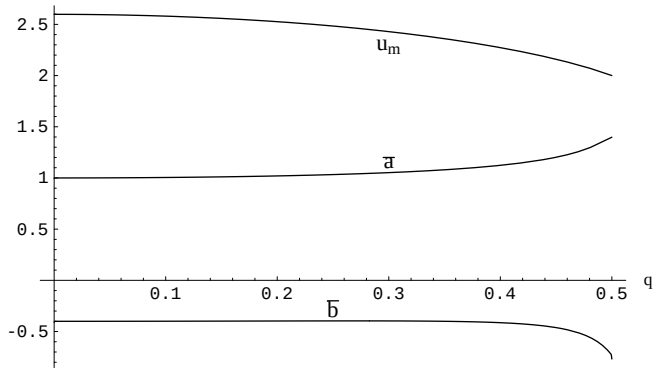

FIG. 3: Coefficients of the strong field limit in Reissner-Nordstrom metric as functions of q.

[16]

$$A(x) = \left(1 - \frac{1}{x}\right)^{\gamma} \tag{63}$$

$$B(x) = \left(1 - \frac{1}{x}\right)^{-\gamma} \tag{64}$$

$$C(x) = \left(1 - \frac{1}{x}\right)^{1-\gamma} x^2 \tag{65}$$

$$\Phi(x) = \frac{q}{2\sqrt{M^2+q^2}}\log\left(1 - \frac{1}{x}\right) \tag{66}$$

$$\gamma = \frac{M}{\sqrt{M^2+q^2}}. \tag{67}$$

where all distances are measured in terms of $x_s = 2\sqrt{M^2+q^2}$ and q is the scalar charge of the central object. This metric admits a photon sphere external to the static limit when $\gamma > \frac{1}{2}$, i.e. when $q < M$. We shall thus restrict our investigations to objects with scalar charge lower than their mass. In Ref. [10], the gravitational lensing of this object was investigated numerically even when

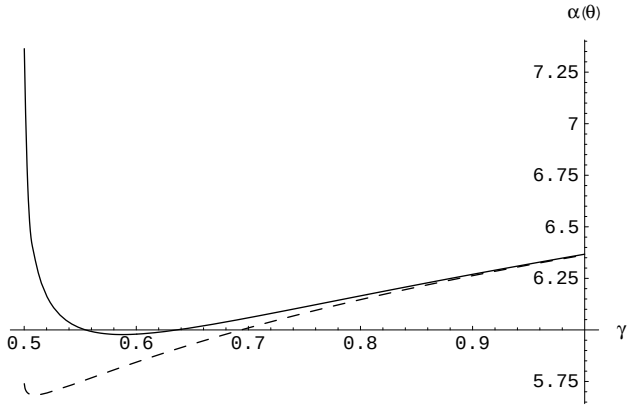

FIG. 4: Deflection angles in a JNW black hole evaluated at $u = u_m + 0.003$ as functions of γ. The solid line is the exact deflection angle; the dashed line is the strong field limit with b_R truncated to first order in γ.

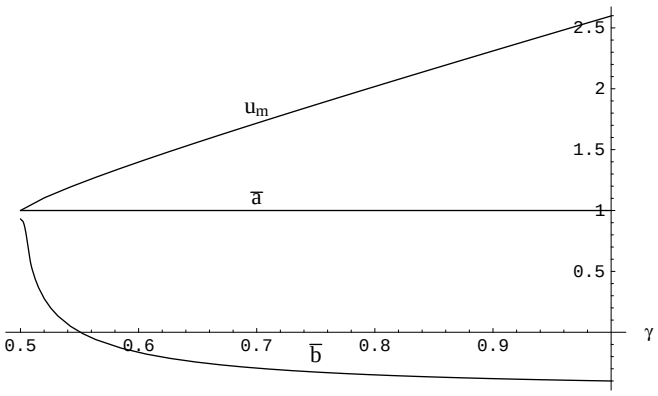

FIG. 5: Coefficients of the strong field limit in a JNW black hole as functions of γ.

$q > M$. In this situation, it was shown that a drastically different and interesting phenomenology shows up.

As in the previous cases, we compute all the coefficients, taking into account that our metric is not written in standard coordinates. The coefficients α and β are

$$\alpha = \left(2 - \frac{2\gamma+1}{x_0}\right) \frac{1}{\gamma x_0^{\gamma-1}} \left[x_0^\gamma - (x_0-1)^\gamma\right] \tag{68}$$

$$\beta = -\frac{(2\gamma+1)(\gamma+1) - 2x_0(3\gamma+1) + 2x_0^2}{(x_0-1)^\gamma} \cdot \cdot \frac{\left[x_0^\gamma - (x_0-1)^\gamma\right]^2}{2\gamma^2 x_0^\gamma}, \tag{69}$$

which easily reduce to Eqs. (43) and (44) when $\gamma = 1$. From the Eq. $\alpha = 0$, we derive the radius of the photon sphere

$$x_m = \frac{2\gamma+1}{2} \tag{70}$$

and then

$$\beta_m = \frac{\left[(2\gamma+1)^\gamma - (2\gamma-1)^\gamma\right]^2}{4\gamma^2 (4\gamma^2-1)^{2\gamma-1}} \tag{71}$$

In the same way as in Reissner-Nordstrom metric, increasing the charge of the central object, the photons are allowed to get closer to the centre. When $\gamma = 0.5$, $x_m = x_s$ and we should change our coordinates frame to perform any significant study.

Here as well we cannot solve the integral (29) exactly. However, we can expand the integrand in powers of $(\gamma-1)$ to get

$$b_R = b_R^0 - 0.1199(\gamma-1) + O(\gamma-1)^2 \tag{72}$$

with b_R^0 given by Eq. (46).

Finally we compute the coefficients of the strong field limit

$$\overline{a} = 1 \tag{73}$$

$$\overline{b} = -\pi + b_R + +2\log\frac{\left[(2\gamma+1)^\gamma - (2\gamma-1)^\gamma\right]^2 (2\gamma+1)}{2\gamma^2 (2\gamma-1)^{2\gamma-1}} \tag{74}$$

$$u_m = \frac{(2\gamma+1)^{\gamma+\frac{1}{2}}}{2(2\gamma-1)^{\gamma-\frac{1}{2}}} \tag{75}$$

Surprisingly, the leading order coefficient $\overline{a}$ is the same as in the Schwarzschild case, in spite of the fact that the radius of the photon sphere has changed.

Once we fix $u - u_m = 0.003$, we see in Fig. 4 that the deflection angle decreases as we increase the charge (decrease γ) until γ reaches the value 0.6, then the deflection angle increases again. The strong field limit, with b_R truncated to first order in γ, at $\gamma = 0.7$ is precise up to 4% in the determination of the outer image.

In Fig. 5, we plot the coefficients of the strong field limit. $\overline{a}$ is constant, $\overline{b}$ increases as γ decreases, but u_m decreases enough to make the deflection angle decrease at constant $u - u_m$ until γ reaches the value 0.6. Comparing with Fig. 3, we can observe that a JNW charge has completely different effects on the strong field limit coefficients than an electric charge and can be identified without confusion.

IV. OBERVABLES IN THE STRONG FIELD LIMIT

In Sect. II we have proved that the strong field limit approximation can be used to obtain a simple and reliable formula for the deflection angle, which contains a logarithmic and a constant term. Now we plug the formula (9) into the lens equation and establish direct relations between the position and the magnification of the

relativistic images and the deflection angle, calculated according to the strong field limit.

The lens equation in the strong field limit was derived in Ref. [8]. It reads

$$\beta = \theta - \frac{D_{LS}}{D_{OS}}\Delta\alpha_n. \tag{76}$$

where D_{LS} is the distance between the lens and the source, $D_{OS} = D_{OL} + D_{LS}$, β is the angular separation between the source and the lens, θ is the angular separation between the lens and the image, $\Delta\alpha_n = \alpha(\theta) - 2n\pi$ is the offset of the deflection angle, once we subtract all the loops done by the photon.

To pass from the deflection angle $\alpha(\theta)$ to the offset $\Delta\alpha_n$, we need to find the values θ_n^0 such that $\alpha(\theta_n^0) = 2n\pi$. Solving Eq. (35) with $\alpha(\theta) = 2n\pi$, we find

$$\theta_n^0 = \frac{u_m}{D_{OL}}\left(1 + e_n\right) \tag{77}$$

$$e_n = e^{\frac{\overline{b} - 2n\pi}{\overline{a}}}. \tag{78}$$

The offset $\Delta\alpha_n$ is then found expanding $\alpha(\theta)$ around $\theta = \theta_n^0$. Letting $\Delta\theta_n = \theta - \theta_n^0$, we find

$$\Delta\alpha_n = -\frac{\overline{a}D_{OL}}{u_m e_n}\Delta\theta_n. \tag{79}$$

The lens equation becomes

$$\beta = \left(\theta_n^0 + \Delta\theta_n\right) + \left(\frac{\overline{a}D_{OL}}{u_m e_n}\frac{D_{LS}}{D_{OS}}\right)\Delta\theta_n. \tag{80}$$

Now we derive the position of all relativistic images, their magnification and the critical curves of the lens.

The second term in the r.h.s. of Eq. (80) is negligible when compared to the last one (since $u_m \ll D_{OL}$). Immediately, we find

$$\theta_n = \theta_n^0 + \frac{u_m e_n\left(\beta - \theta_n^0\right)D_{OS}}{\overline{a}D_{LS}D_{OL}}. \tag{81}$$

where the correction to θ_n^0 is much smaller than θ_n^0.

This formula is valid both for the images on the same side of the source and the images on the opposite side. In fact, to find the latter, it is sufficient to take a negative β in Eq. (81).

Finally, we have expressed the position of the relativistic images in terms of the coefficients $\overline{a}$, $\overline{b}$ and u_m. If we manage to determine these coefficients from the observation of the relativistic images, we are rewarded with information about the parameters of the black hole stored in them.

The critical curves are just Einstein rings corresponding to a source perfectly aligned with the lens. Their radius is obtained putting $\beta = 0$ in (81).

Another important source of information is the magnification of the images which is the inverse of the Jacobian evaluated at the position of the image. For simplicity, we approximate the position of the images by θ_n^0, recalling that the correction provided by Eq. (81) is negligible.

$$\mu_n = \left.\frac{1}{\frac{\beta}{\theta}\frac{\partial\beta}{\partial\theta}}\right|_{\theta_n^0}. \tag{82}$$

We have

$$\left.\frac{\partial\beta}{\partial\theta}\right|_{\theta_n^0} = 1 + \frac{\overline{a}D_{OL}}{u_m e_n}\frac{D_{LS}}{D_{OS}}. \tag{83}$$

where the first term is small compared to the second and can be neglected.

Finally, the magnification is

$$\mu_n = \frac{1}{\left|detJ|_{\theta_n^0}\right|} = \frac{\theta_n^0}{\beta\left.\frac{\partial\beta}{\partial\theta}\right|_{\theta_n^0}} = e_n\frac{u_m^2\left(1+e_n\right)D_{OS}}{\overline{a}\beta D_{OL}^2 D_{LS}}, \tag{84}$$

which decreases very quickly in n.

Formulae (77) and (84) relate the position and the magnification to the strong field limit coefficients. The successive step is to solve the inversion problem, i.e. we have to find out the most effective way to go back from measured positions and fluxes to the strong field limit coefficients, which carry the information about the nature of the black hole.

The minimum impact parameter can be simply obtained as

$$u_m = D_{OL}\theta_\infty \tag{85}$$

where θ_∞ represents the asymptotic position approached by a set of images, obtained by Eq. (77) in the limit $n \to \infty$.

To obtain the coefficients $\overline{a}$ and $\overline{b}$, we need to separate at least the outermost image from all the others. We shall thus consider the simplest situation where only the outermost image θ_1 is resolved as a single image, while all the remaining ones are packed together at θ_∞.

Our observables will thus be

$$s = \theta_1 - \theta_\infty \tag{86}$$

$$r = \frac{\mu_1}{\sum_{n=2}^{\infty}\mu_n}, \tag{87}$$

which respectively represent the separation between the first image and the others, and the ratio between the flux of the first image and the flux coming from all the other images.

The sum of the fluxes of all the set of relativistic images except the first is

$$\sum_{n=2}^{\infty}\mu_n = \frac{u_m^2 D_{OS}e^{\frac{\overline{b}}{\overline{a}}}}{\overline{a}\beta D_{OL}^2 D_{LS}}\frac{e^{\frac{4\pi}{\overline{a}}} + e^{\frac{2\pi}{\overline{a}}} + e^{\frac{\overline{b}}{\overline{a}}}}{e^{\frac{4\pi}{\overline{a}}} - 1}. \tag{88}$$

We can notice that $e^{\frac{2\pi}{\overline{a}}} \gg 1$ and $e^{\frac{\overline{b}}{\overline{a}}}$ is of order one, since $\overline{a}$ and $\overline{b}$ are of order one too. Using these simple observations, we can simplify our formulae to have

$$s = \theta_\infty e^{\frac{\overline{b}}{\overline{a}} - \frac{2\pi}{\overline{a}}} \tag{89}$$

$$r = e^{\frac{2\pi}{\overline{a}}}. \tag{90}$$

These two formulae can be easily inverted to give

$$\overline{a} = \frac{2\pi}{\log r} \tag{91}$$

$$\overline{b} = \overline{a} \log\left(\frac{rs}{\theta_\infty}\right). \tag{92}$$

Finally, just measuring an angular separation and a flux ratio, we are able to reconstruct the full strong field limit expansion of the deflection angle for the observed gravitational lens.

The coefficients of the strong field limit are constrained by the characteristics of the metric to be well precise real numbers. Thus, if strong field gravitational lensing will be detected, comparing the experimental coefficients with the theoretical expectations, calculated according to different models, we are able to identify the nature of the lensing black hole unambiguously.

A. A numerical example: lensing by the galactic supermassive black hole

It is significant to consider a realistic case where we can discuss the instrumental sensitivity required to detect relativistic images and possibly distinguish between different black holes through the reconstruction of the strong field limit coefficients.

The centre of our galaxy is believed to host a black hole with mass $M = 2.8 \times 10^6 M_\odot$ [17]. The lensing of a background source by this supermassive black hole was discussed in detail by Virbhadra & Ellis [6]. Taking $D_{OL} = 8.5$kpc as the distance between the sun and the center of Galaxy, they found that the separation between each set of relativistic images with respect to the central lens would be $\theta_\infty \sim 17$ microarcsecs. In principle, such a resolution is reachable by actual VLBI projects, but we must be aware that the disturbances intrinsic in such observations (mainly due to extinction and emission by accreting matter), would make the identification of the relativistic images very difficult, as already pointed out in Ref. [6].

In Tab. I, following this line, we estimate the quantities we need for a complete strong field limit reconstruction in different situations, starting from a simple Schwarzschild black hole and then going to black holes with different values of the electric charge and JNW charge.

Looking at Tab. I, we can make some considerations of different order. Indeed, the easiest parameter to evaluate is the minimum impact parameter u_m, since a microarcsec resolution is reachable in the next years. This information alone, can already distinguish between a Schwarzschild or other types of geometry. In fact, since the total mass and the distance of the black hole are known to a reasonable accuracy (and possibly will be even better fixed in the next years), an u_m smaller than predicted would signal that the structure of spacetime close to the central black hole is not described by Schwarzschild solution. On the other hand, if u_m is compatible within experimental uncertainties with Schwarzschild case, we would set an upper limit for the parameters describing other black holes, such as an electric or a scalar charge.

In a second extent, to fit all the strong field limit coefficients into any black hole model, we need to separate at least the outermost relativistic image from the others. We see that this can be done only increasing optical resolution at least by two orders of magnitude with respect to actual observational projects. Therefore, with these numbers, it seems that we are forced to wait for further technological developments. However, given the evolution rate of astronomical facilities in the last twenty years, it is not unthinkable that these two orders of magnitude will be reached within a not so far future.

Black holes are also present in the bulge of other galaxies. As far as we have investigated, in the best cases, the instrumental resolutions needed for strong field gravitational lensing are about the same as for the Milky Way black hole. So, the determination of u_m by next future observations would possibly confirm or disprove Schwarzschild geometry for several extra-galactic black holes too. The complete determination of the strong field limit coefficients instead remains a long term project, unless more favourable astrophysical situations emerge.

V. SUMMARY

Gravitational lensing is undoubtedly a potential powerful tool for the investigation of strong fields. By general arguments we have shown that the deflection angle diverges logarithmically as we approach the photon sphere. We have drawn a general method to compute the coefficient of the leading order divergent term and the first regular term. When the latter cannot be calculated analytically, we have seen that it can be well approximated by a simple series expansion starting from Schwarzschild spacetime.

We have applied our method to Schwarzschild, Reissner-Nordstrom and Janis-Newman-Winicour black hole, explicitly calculating and plotting the strong field limit coefficients.

Of course, it is possible to apply the strong field limit, in the form given in this paper, to any spherically symmetric metric representing a black hole. In this way, it is possible to compare the gravitational lensing behaviour of these objects in different theories of gravitation. In principle, the extension to non-spherically symmetric and rotating black holes is possible. However, the dependence of the deflection angle on more than one variable can put severe obstacles in the way of analytic solutions of the

	Schwarzschild	Reissner - Nordstrom				Janis-Newman-Winicour			
		$q = 0.1$	$q = 0.2$	$q = 0.3$	$q = 0.4$	$\gamma = 0.9$	$\gamma = 0.8$	$\gamma = 0.7$	$\gamma = 0.6$
θ_∞ (μarcsecs)	16.87	16.76	16.41	15.78	14.76	16.67	16.38	15.93	15.13
s (μarcsecs)	0.0211	0.0216	0.0234	0.0275	0.038	0.0213	0.0216	0.0222	0.0239
r_m (magnitudes)	6.82	6.79	6.69	6.49	6.07	6.82	6.82	6.82	6.82
u_m/R_S	2.6	2.58	2.53	2.43	2.27	2.57	2.52	2.45	2.33
$\overline{a}$	1	1.005	1.02	1.052	1.123	1	1	1	1
$\overline{b}$	-0.4002	-0.3993	-0.3972	-0.3965	-0.4136	-0.3808	-0.35	-0.2945	-0.1659

TABLE I: Estimates for the main observables and the strong field limit coefficients for the black hole at the center of our galaxy in different hypotheses for the spacetime geometry. θ_∞ and s are defined in the text; r_m is r converted to magnitudes: $r_m = 2.5$ Log r; u_m, $\overline{a}$ and $\overline{b}$ are the strong field limit coefficients; $R_S = \frac{2GM}{c^2}$ is the Schwarzschild radius.

problem. Nevertheless, this is indeed another important point which needs to be investigated to complete the picture of black hole lensing.

Differences in the deflection angle are immediately reflected on the relativistic images. If the mass and the distance of the lens is known, then the detection of any set of relativistic images would immediately check the Schwarzschild geometry. VLBI should be able to provide an observational answer, if the relativistic images are not hidden behind environmental noise.

Furthermore, if the outermost image is resolved from the others, it is then possible to fully reconstruct the strong field limit coefficients and select a precise black hole model. Our present observational facilities are not so far from the required resolutions, which, for the galactic black hole, are of the order of 0.01 microarcsecs. As a long term project the detection of the outermost image stands as a very interesting, non-trivial challenge for future technology.

Strong field limit represents an important step in the construction of a robust theoretical scheme connecting the gravitational lensing with the strong field properties. By a simple and reliable expansion, it clarifies the whole phenomenology and the differences between various models that should be expected in the appearance of relativistic images. If these so elusive features will be detected, we will finally have a way to effectively discriminate between alternative theories of gravitation and grow in our knowledge of spacetime.

Acknowledgments

I would like to thank Gaetano Lambiase and Salvatore Capozziello for helpful comments and discussions.

[1] A. Einstein, Science, 84 (1936) 506.
[2] P. Schneider, J. Ehlers, E.E. Falco, Gravitational lenses, Springer-Verlag, Berlin (1992).
[3] S.U. Viergutz, A&A 272 (1993) 355.
[4] J.M. Bardeen, Black Holes, ed. C. de Witt & B.S. de Witt, NY, Gordon & Breach, 215 (1973).
[5] H. Falcke, F. Melia, E. Agol, ApJ Letters 528 (1999) L13.
[6] K.S. Virbhadra, G.F.R. Ellis, Phys. Rev. D62 (2000) 084003.
[7] S. Frittelli, T.P. Kling, E.T. Newman, Phys. Rev. D 61 (2000) 064021
[8] V. Bozza, S. Capozziello, G. Iovane & G. Scarpetta, Gen. Rel. and Grav. 33 (2001) 1535.
[9] E.F. Eiroa, G.E. Romero, D.F. Torres, gr-qc/0203049.
[10] K.S. Virbhadra, G.F.R. Ellis, Phys. Rev. D65 (2002) 103004.
[11] Constellation-X web page: constellation.gsfc.nasa.gov; Maxim web page: maxim.gsfc.nasa.gov; J.S. Ulvestad astro-ph/9901374.
[12] C.-M. Claudel, K.S. Virbhadra, G.F.R Ellis, J. Math. Phys. 42 (2001) 818.
[13] S. Weinberg, Gravitation and cosmology: principles and applications of the general theory of relativity, John Wiely & Sons, NY 1972.
[14] B. Carter, Phys. Rev. 174 (1968) 1559.
[15] S.W. Hawking, G.F. Ellis, The large scale structure of space-time, Cambridge University Press, 1973.
[16] A. Janis, E. Newman, J. Winicour, Phys. Rev. Lett. 20 (1968) 878; M. Wyman, Phys. Rev. D 24 (1985) 839; R. Gautreau, Nuovo Cimento B 62 (1969) 360.
[17] D. Richstone et al., Nature, 395 (1998) A14.